

Reflectivity cross plot of Modified Zoeppritz Equation

ABSTRACT

Beside the complexities and not readily practical applications resulting from the full Zoeppritz equation, the seismic amplitude reflection does not give enough information beyond the critical angle. Consequently, there are breakdown of the Zoeppritz equation approximations at angle of incidence beyond 30° (Shuey's approximation). More so, the validity is only for slight contrast in elastic parameters across the formations and small angle of incidence is assumed. In an attempt to address these inaccuracies and enhance understanding of seismic reservoir responses and prediction of fluid and lithology, a modified form of the Zoeppritz equation is derived using relations between elastic constants and velocities in terms of Pseudo Poisson' ratio reflectivity, rigidity reflectivity, density reflectivity in linearized forms devoid of the complexities associated with the original Zoeppritz equation with practical applications in hydrocarbon exploration, exploitation and production. These properties are lithology and fluid discriminators. The modified Zoeppritz equation was analyzed using well data from oil field in a sedimentary basin, onshore of Niger Delta area. Reflectivity crossplot was carried out and comparison with the exact and other approximations was done to validate the derived equation. The results showed that the modified equation can be applied in exploration beyond the critical angle than the shuey's and Aki & Richard's approximations especially for deep targets and wide angle acquisition for accurate estimation of intercept and gradient attributes. The modified Zoeppritz equation in this study gives higher accuracy at far offset than the two foremost approximations.

Keywords: [Put four to eight keywords } (Arial, inclined, 10 font, justified)

1. INTRODUCTION

The Zoeppritz equations are complicated, complex and non-linear that an intuitive understanding of how the variations of amplitude are related to different rock properties was not readily apparent [1]. Through the years, some linearized approximations to the Zoeppritz equations had been made, which make the interpretation extra intuitive [2].

A number of modifications to the full Zoeppritz equation that have been linearized can be reviewed based on their different emphasis. Starting from the equation of [3], which emphasis are on the fluid and rigidity properties, providing insight to fluid substitution interpretation. [4] looked at the contrast in the compressional (P-wave) and Shear (S- wave) velocities and density, while [5] relates the amplitude contrast to changes in Poisson's ratio, compressional (P-wave) velocity, and density [6]. The Primary wave and Secondary wave

velocity reflectivities were deduced from the equation given by [7] from which they derived the fluid factor [6, 8]. [9] gives us a direct estimation of P-wave impedance and S-wave impedance, based on which [10] proposed Lambda –Mu-Rho (LMR) method and in 1995, [11] approximation was used to derive P-wave reflectivity and Poisson's reflectivity. The equation from [12] was used for the extraction of Lambda reflectivity $\Delta\lambda/\lambda$, Mu reflectivity $\Delta\mu/\mu$, and bulk modulus reflectivity $\Delta K/K$, and the lead to [13] given an approximation to take care of the inaccuracy of the V_s/V_p ratio which affects the inversion process in [12]. This study aims at analyzing and modifying Zoeppritz Equation to enhance characterization of lithology and discrimination of fluid in a typical Niger delta hydrocarbon reservoir terms of shear modulus, Pseudo-Poisson's ratio, and density with the generation of reflectivity curves for incidence angles 0° to 90° to validate the modified equation.

The General Linearized Approximation to Zoeppritz Equation

[14] Russell *et al.*, 2006 summarized several Zoeppritz equation that was linearized based on their different emphasis into a three term equation as:

$$R(\theta) = aR_1 + bR_2 + cR_3 \quad 1$$

R_i are reflectivity terms for the rock properties, the incident angle and $(V_p/V_s)^2$ are functions of coefficients a, b, and c [6, 14]. This equation generalizes the linearized approximations and summarized in Table 1 and Table 2

2. MATERIAL AND METHODS

[4] equation was rearranged in terms of Pseudo Poisson' ratio reflectivity $\frac{\Delta q}{q}$, rigidity reflectivity $\frac{\Delta\mu}{\mu}$, and density reflectivity $\frac{\Delta\rho}{\rho}$. These properties are lithology and fluid discriminators [15].

$$R_P(\theta) = \frac{1}{2} \left[\frac{\Delta V_P}{V_P} + \frac{\Delta\rho}{\rho} \right] - 2 \left(\frac{V_S}{V_P} \right)^2 \left[\frac{2\Delta V_S}{V_S} + \frac{\Delta\rho}{\rho} \right] \sin^2\theta + \frac{1}{2} \frac{\Delta V_P}{V_P} \tan^2\theta \quad 2$$

$$R_P(\theta) = \frac{1}{2} \left(\frac{\Delta V_P}{V_P} - \frac{\Delta V_S}{V_S} \right) (1 + \tan^2\theta) + \frac{1}{2} \frac{\Delta V_S}{V_S} \left(\sec^2\theta - 8 \left(\frac{V_S}{V_P} \right)^2 \sin^2\theta \right) + \frac{1}{2} \frac{\Delta\rho}{\rho} \left(1 - 4 \left(\frac{V_S}{V_P} \right)^2 \sin^2\theta \right) \quad 3$$

According to [2] and [16], the Pseudo Poisson's ratio is defined as:

$$\frac{\Delta q}{q} \equiv \frac{\Delta(V_P/V_S)}{V_P/V_S} = \frac{\Delta(I_P/I_S)}{I_P/I_S} = \frac{\Delta V_P}{V_P} - \frac{\Delta V_S}{V_S} = \frac{\Delta I_P}{I_P} - \frac{\Delta I_S}{I_S} \quad 4$$

Therefore, substitute equation 4 into equation 3,

Table 1: R_i terms for the general linearized equation [6, 14]

Approximations	R_1	R_2	R_3	Assumption
Aki-Richards (1980)	$\frac{\Delta V_P}{V_P}$	$\frac{\Delta V_S}{V_S}$	$\frac{\Delta\rho}{\rho}$	From Bortfeld's approximation
$(V_P V_S \rho)$	V_P	V_S	ρ	

Shuey, (1985) ($\rho V_p, \sigma, V_p$)	$\frac{1}{2} \left[\frac{\Delta V_p}{V_p} + \frac{\Delta \rho}{\rho} \right]$	$\left[\frac{1}{2} \frac{\Delta V_p}{V_p} - \frac{\Delta V_s}{V_s} - \frac{1}{2} \frac{\Delta \rho}{\rho} \right]$	$\frac{1}{2} \frac{\Delta V_p}{V_p}$	The third term can be ignored for $\theta > 30^\circ$; Assume $V_s/V_p = 0.5$
Smith and Gidlow (1987) ($V_p V_s \rho$)	$\frac{\Delta V_p}{V_p}$	$\frac{\Delta V_s}{V_s}$	$\frac{1}{2} \frac{\Delta V_p}{V_p}$	Gardner's relationship for density; No assumption for incident angle
Fatti et al. (1994) ($\rho V_p, \rho V_s, \rho$)	$\frac{\Delta I_p}{I_p}$	$\frac{\Delta I_s}{I_s}$	$\frac{\Delta \rho}{\rho}$	The third term can be ignored for $\theta > 30^\circ$
Hilterman (1995) ($\rho V_p, \sigma$)	$\frac{\Delta I_p}{I_p}$	$\frac{\Delta \sigma}{(1 - \sigma)^2}$	0	From Shuey's approximation Assume $V_s/V_p = 0.5$
Gray (1999) ($\lambda \mu \rho$)	$\frac{\Delta \lambda}{\lambda}$	$\frac{\Delta \mu}{\mu}$	$\frac{\Delta \rho}{\rho}$	No assumption
Gray (1999) ($K \mu \rho$)	$\frac{\Delta K}{K}$	$\frac{\Delta \mu}{\mu}$	$\frac{\Delta \rho}{\rho}$	No assumption
Samba and Jiangpiang (2011) ($\lambda Q \rho$)	$\frac{\Delta \lambda}{\lambda}$	$\frac{\Delta Q}{Q} = \frac{\Delta \lambda}{\lambda} - \frac{\Delta \mu}{\mu}$	$\frac{\Delta \rho}{\rho}$	From Gray's approximation Assume $V_s/V_p = 0.5$

Table 2: Terms a, b, and c for the general linearized equation [6, 14]

Approximations	a	b	c
Aki-Richards (1980) ($V_p V_s \rho$)	$\frac{1}{2} (1 + \tan^2 \theta)$	$4 \frac{V_s^2}{V_p^2} \sin^2 \theta$	$\frac{1}{2} \left(1 - 4 \frac{V_s^2}{V_p^2} \sin^2 \theta \right)$
Shuey, 1985 ($\rho V_p, \sigma, V_p$)	1	$\sin^2 \theta$	$\tan^2 \theta - \sin^2 \theta$
Smith and Gidlow (1987) ($V_p V_s \rho$)	$\frac{5}{8} - 1/2 (V_s^2/V_p^2) \sin^2 \theta + 1/2 \tan^2 \theta$	$-4 (V_s^2/V_p^2) \sin^2 \theta$	$\tan^2 \theta$
Fatti et al. (1994) ($\rho V_p, \rho V_s, \rho$)	$(1 + \tan^2 \theta)$	$-4 \left(\frac{V_s}{V_p} \right)^2 \sin^2 \theta$	$-\left(\frac{1}{2} \tan^2 \theta - 2 \left(\frac{V_s}{V_p} \right)^2 \sin^2 \theta \right)$
Hilterman (1995) ($\rho V_p, \sigma$)	$\cos^2 \theta$	$\sin^2 \theta$	0
Gray (1999) ($\lambda \mu \rho$)	$\left[\frac{1}{4} - 2 \left(\frac{\beta}{\alpha} \right)^2 \right] \sec^2 \theta$	$\left(\frac{\beta}{\alpha} \right)^2 \left[\frac{\sec^2 \theta}{2} - 2 \sin^2 \theta \right]$	$\left[\frac{1}{2} - \frac{1}{4} \sec^2 \theta \right]$
Gray (1999) ($K \mu \rho$)	$\left[\frac{1}{4} - \frac{1}{3} \left(\frac{\beta}{\alpha} \right)^2 \right] \sec^2 \theta$	$\left(\frac{\beta}{\alpha} \right)^2 \left[\frac{\sec^2 \theta}{3} - 2 \sin^2 \theta \right]$	$\left[\frac{1}{2} - \frac{1}{4} \sec^2 \theta \right]$
Samba and Jiangpiang (2011) ($\lambda Q \rho$)	$\left[\frac{\sec^2 \theta}{4} - 2K \sin^2 \theta \right]$	$\left(\frac{\beta}{\alpha} \right)^2 \left[2K \sin^2 \theta - \frac{1}{2} \sec^2 \theta \right]$	$\frac{1}{4} [1 - \tan^2 \theta]$

$$R_p(\theta) = \frac{1}{2} \frac{\Delta q}{q} (1 + \tan^2 \theta) + \frac{1}{2} \frac{\Delta V_s}{V_s} \left(\sec^2 \theta - 8 \left(\frac{V_s}{V_p} \right)^2 \sin^2 \theta \right) + \frac{1}{2} \frac{\Delta \rho}{\rho} \left(1 - 4 \left(\frac{V_s}{V_p} \right)^2 \sin^2 \theta \right) \quad 5$$

Moreso, [17] gave $\Delta \mu$ as

$$\Delta \mu = V_s^2 \Delta \rho + 2 \rho V_s \Delta V_s \quad 6$$

Therefore, Equation 5 can be rewritten as

$$R_P(\theta) = \frac{1}{2} \frac{\Delta q}{q} (1 + \tan^2 \theta) + \frac{1}{2} \frac{\Delta \mu}{\mu} \left(\frac{\sec^2 \theta}{2} - 4 \left(\frac{V_S}{V_P} \right)^2 \sin^2 \theta \right) + \frac{1}{2} \frac{\Delta \rho}{\rho} \left(1 - \frac{1}{2} \sec^2 \theta \right) \quad 7$$

Equation 7 is the modified Zoeppritz equation [19, 20]

3. RESULTS AND DISCUSSION

The results of P-P reflectivity from the modified Zoeppritz equation were crossplotted against incidence angles $0^\circ - 90^\circ$ and compared with the exact Zoeppritz equation and other approximations.

A comparison of results obtained from P-P reflectivity coefficient versus incident angle for shale over gas sand and shale over oil sand scenarios, using the exact Zoeppritz, Aki-Richards and Modified Zoeppritz Equations of P-P reflectivity coefficient with respect to angle of incidence as shown in Figure 1

The rock properties for shale over oil sand scenario used for this plot are:

- P-wave velocities: in shale 2650 m/s, and in oil sand 2560m/s
- S-wave velocities: in shale 1150 m/s, and in oil sand 1180m/s
- Densities : in shale 2.48 g/cc , and in oil sand 2.23 g/cc

The rock properties for shale over gas sand scenario used for this plot are:

- P-wave velocities: in shale 2650 m/s, and in gas sand 2340m/s
- S-wave velocities: in shale 1150 m/s, and gas sand 1180m/s
- Densities : in shale 2.48 g/cc, and in gas sand 2.16 g/cc

Figure 1 is a plot of shale over gas sand and shale over oil sand scenarios. There are both Class III AVO responses, having normal reflectivity amplitude R_0 negative and increases with increasing angle/offset. The AVO plot shale over gas sands response exhibit a negative zero-offset reflection coefficient (≈ -0.1311), while shale over oil sand response exhibit a negative zero- degree offset reflection coefficient (≈ -0.0703).

The reflectivity for shale over gas sand is high than shale over oil sand in each of the plots. This by implication implies larger reflection amplitudes for shale over gas sand than shale over oil sand. The fit is better and well pronounced for shale over oil sand plot.

The plot shows that Zoeppritz's equation, Aki and Richard's approximation and the modified equation fit each other near the critical angle 25° while that of Zoeppritz and the modified equation fit well beyond 25° . This could be attributed to the sensitivity of the elastic parameters in the modified equation which are fractional contrast of Pseudo Poisson' ratio reflectivity $\frac{\Delta q}{q}$, rigidity reflectivity $\frac{\Delta \mu}{\mu}$, and density reflectivity $\frac{\Delta \rho}{\rho}$.

A comparison of results obtained for a gas sand over shale reflection for Shuey's approximation and modified equation for P-P reflection coefficient with respect to angle of incidence as shown in Figure 2

The rock properties for gas over shale sand scenario used for this plot are:

- P-wave velocities: in gas sand 1650 m/s, in shale 3240m/s
- S-wave velocities: in gas sand 1090 m/s, in shale 1620m/s
- Densities: in gas sand 2.07 g/cm^3 , in shale 2.34 g/cm^3

The gas over shale formation in Figure 2 at zero offset starts with slightly negative reflection coefficient, it becomes less negative as the offset increases for gas over shale reflectivity generated from Shuey's equation with a phase change at less than 30° angle of incidence. On the other hand, the reflectivity generated from the modified equation increase in amplitude slightly with a phase change occurring at less than 40° angle of incidence. The

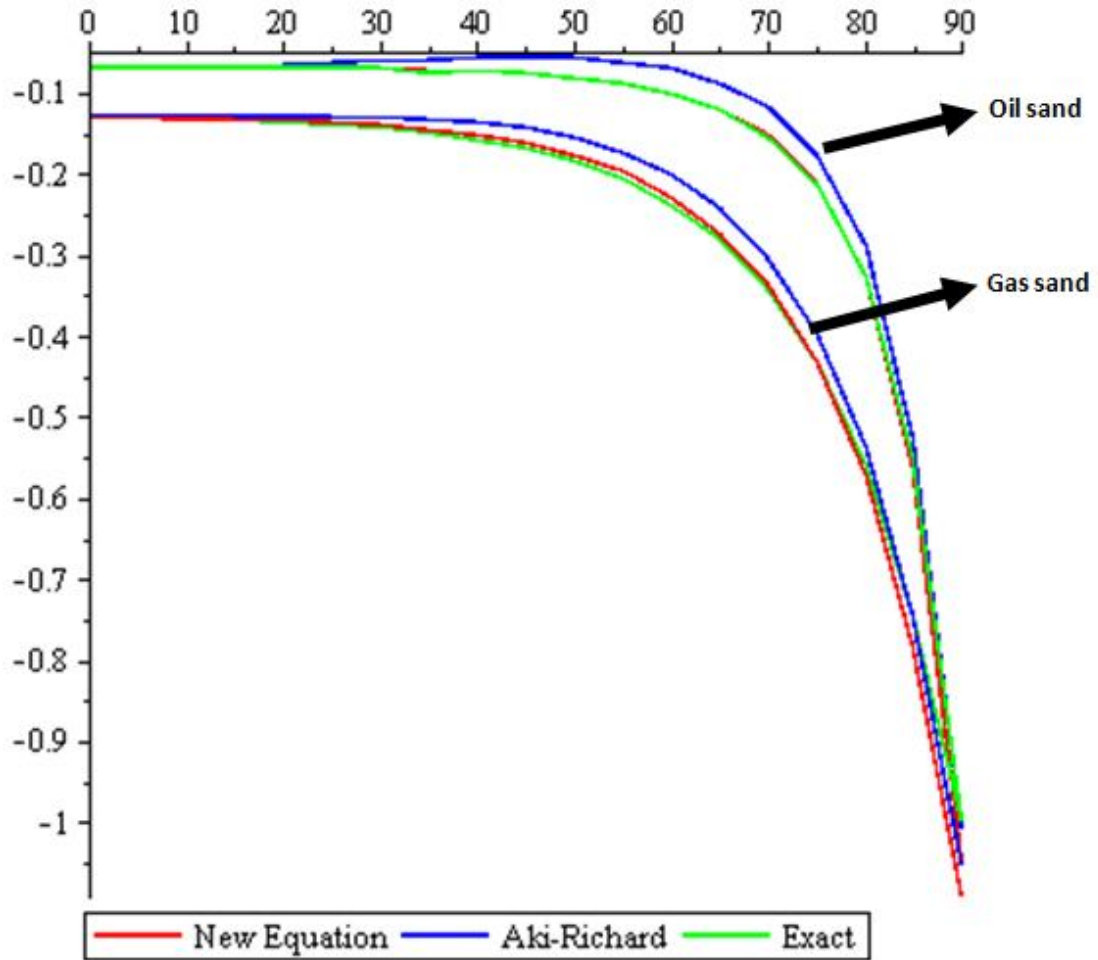


Fig. 1: Comparison of angle reflection coefficients, $R_{pp}(\theta)$ obtained from Exact Zoeppritz equation, Aki-Richards and the new Approximation for Class III Shale over Gas sand and Shale over Oil sand for a range of incidence angles from 0 to 90°

Shuey's and the modified equation show the same fit at the near angle of incidence with a negative zero-offset reflection coefficient (≈ -0.0983).

From the plot it was observed that the Shuey's approximation breaks down before the critical angle showing the inadequacy of the approximation while the modified equation is stable at angles above the critical angle 30°. This could be attributed to the sensitivity of the elastic parameters in the modified equation which are fractional contrast of Pseudo Poisson' ratio reflectivity $\frac{\Delta q}{q}$, rigidity reflectivity $\frac{\Delta \mu}{\mu}$, and density reflectivity $\frac{\Delta \rho}{\rho}$. Therefore, the modified equation can be used to explore at increasing angle/offset beyond the critical angle than the shuey's approximation

The modified equation has reflectivity at increasing angle of incidence $R(\theta)$ slightly less negative than Shuey's approximation. Shuey's approximation is best at incident angle less than 30°, while the modified equation is best at incident angle less than 60° before the second phase reversal.

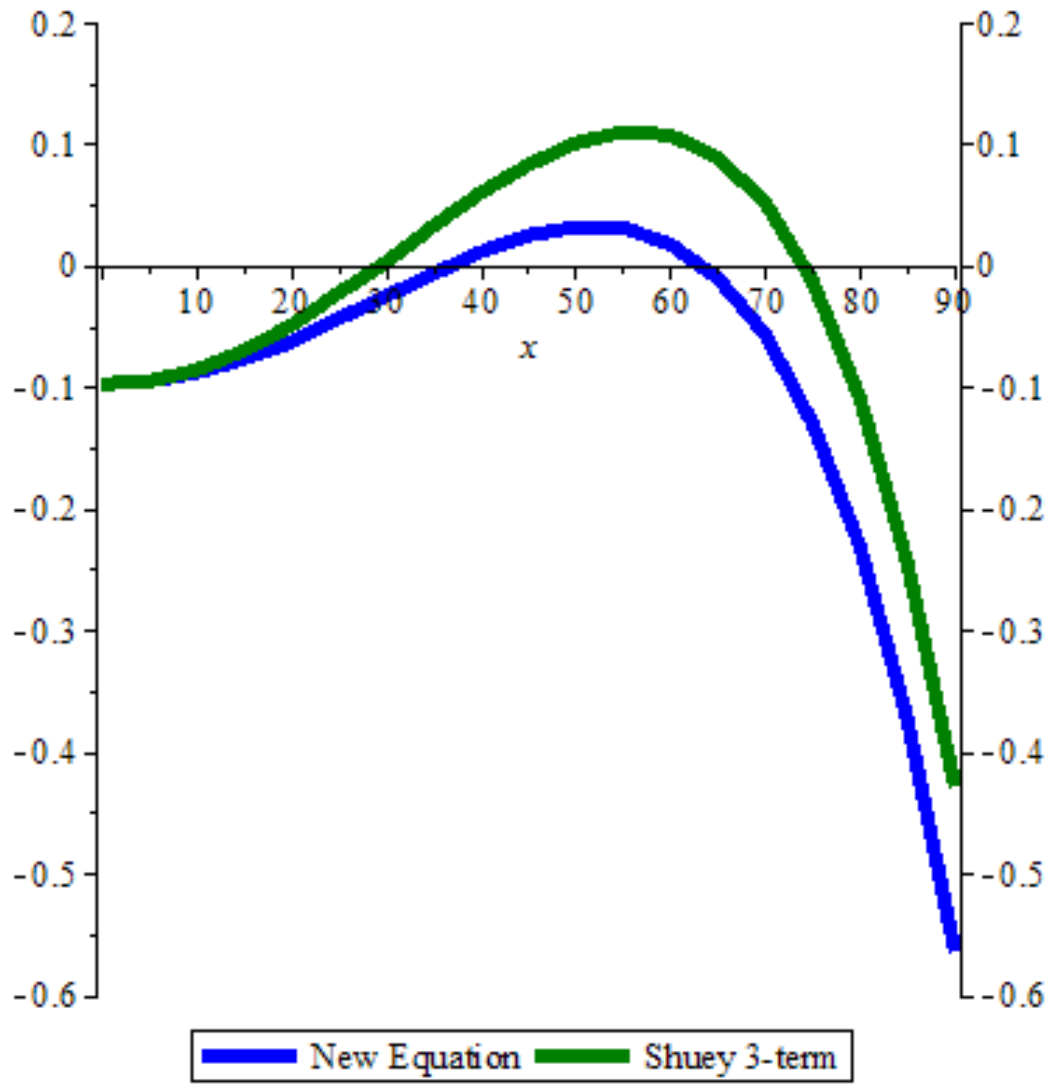


Fig. 2: Comparison of angle reflection coefficient, $R_{PP}(\theta)$ obtained from the new approximation and Shuey's approximation for Class II Gas sand over Shale for a range of incidence angles from 0 to 90° .

4. CONCLUSION

This study shows a modification of the P – P wave reflectivity coefficients in form of Pseudo Poisson' ratio reflectivity $\frac{\Delta q}{q}$, rigidity reflectivity $\frac{\Delta \mu}{\mu}$, and density reflectivity $\frac{\Delta \rho}{\rho}$ as a function of the fundamental elastic parameters of the subsurface. This modified equation has three terms like the Aki-Richard and Shuey (three terms) equations but is more stable and has higher accuracy at far offset (above the critical angle).

In conclusion, the modified Zoeppritz equation in this study gives higher accuracy at far offset than the two foremost approximations.

REFERENCES

Mahmoudian F, Margrave GF. P-wave impedance, S-wave impedance and density from linear AVO inversion: Application to VSP data from Alberta. CREWES Research Report. 18; 2006

Feng H, Bancroft JC. AVO principles, processing and inversion CREWES Research Report — 18; 2006

Bortfeld R. Approximations to the reflection and transmission coefficients of plane longitudinal and transverse waves: Geophysical Prospecting. 1961;9:485-502.

Aki KI, Richards PG. Quantitative seismology - Theory and methods, W. H. Freeman and Company, San Francisco. I, 5.2; 1980

Shuey RT. A simplification of the Zoeppritz Equations: Geophysics. 1985;50:609 – 614.

Feng H. Hydrocarbon indicators derived from AVO analysis (Master Thesis). University of Calgary, Canada. 2009

Smith GC, Gidlow PM. Weighted stacking for rock property estimation and detection of gas: Geophysical Prospecting. 1987;35:993-1014.

Larsen JA. AVO Inversion by Simultaneous P-P and P-S Inversion (Masters Thesis), University of Calgary, Canada. Consortium for Research in Elastic Wave Exploration Seismology. 1999

Fatti JL, Smith GC, Vail PJ, Strauss PJ, Levitt PR. (1994). Detection of gas in sandstone reservoirs using AVO analysis: A 3-D seismic case history using the Geostack technique: Geophysics. 1994;59:1362-1376.

Goodway W, Chen T, Downton J. Improved AVO Fluid detection and lithology discrimination using lame petrophysical parameters, from P- and S- inversion. CSEG. 1997;148-151.

Hilterman F, Verm R. Lithology color-coded seismic sections: The calibration of AVO cross-plotting to rock properties. The Leading Edge. 1995;14(8):847-853.

Gray D, Goodway W, Chen T. Bridging the gap: Using AVO to detect changes in fundamental elastic constants: SEG meeting abstracts. 1999;852-855.

Samba CP, Jiangping L. (2011). The Direct Inversion of λ/μ from Elastic Impedance. Journal of American Science. 2011;7(3):317-321.

Russell BH, Hampson D, Bankhead B. An Inversion Primer, CSEG *Reorder, Special Edition*. 2006; 96-103.

Pengyuan S, Xiuli L, Yanpeng L, Yuanyuan Y. Haifeng C. Elastic parameter AVO approximations and their applications: BGP, CNPC SEG Las Vegas Annual Meeting. 2008;523-527.

Almutlaq MH, Margrave GF. Tutorial: AVO inversion, CREWES Research Report — 22. 2010

Ma J. Morozov IB. Ray-path elastic impedance, CSEG National Convention Great Explorations – Canada and Beyond. 2004;10-12.

Balogun AO. Ebeniro JO, Evaluation of Seismic Attributes Generated from Extended Elastic Impedance for Lithology and Fluid Discrimination, International Journal of Science and Research (IJSR). 2017;6(9):776 – 779.

Balogun AO. Ehirim CN, Lithology and Fluid Discrimination Using Bulk Modulus and Mu-Rho Attributes Generated From Extended Elastic Impedance, International Journal of Science and Research (IJSR). 2017;6(10):639 – 643.

UNDER PEER REVIEW